Astron. Astrophys. 358, 57–64 (2000)

ASTRONOMY AND ASTROPHYSICS

Can star collisions explain the AGN variability?

G. Torricelli-Ciamponi[1,2], **C. Foellmi**[1,3], **T.J.-L. Courvoisier**[1,4], **and S. Paltani**[1,4]

[1] *INTEGRAL* Science Data Centre, ch. d'Ecogia 16, 1290 Versoix, Switzerland
[2] Osservatorio Astrofisico di Arcetri, L.E. Fermi 5, 50125 Firenze, Italy
[3] Université de Montréal,Département de physique, Montréal (Québec) H3C 3J7, Canada
[4] Geneva Observatory, ch. des Maillettes 51, 1290 Versoix, Switzerland

Received 23 August 1999 / Accepted 7 March 2000

Abstract. Star collisions may easily occur in a cluster of stars orbiting around a massive black hole. Such collisions can transform part of the star kinetic energy in observable radiating energy. In this paper we derive the star collision rate and the resulting highly variable luminosity for the case of a cluster containing stars of different masses. The variability of the derived light curves is computed for different sets of parameters and compared to the available data (Paltani & Courvoisier 1997). The comparison shows that the observed data trend can be reproduced by this model.

Key words: galaxies: active – galaxies: nuclei – galaxies: quasars: general – ultraviolet: galaxies

1. Introduction

In the last years much attention has been devoted to the analysis of active galactic nuclei (AGN) ultraviolet variability. In particular the relationship between variability and luminosity in quasars and in Seyfert galaxies has been investigated by many authors (see Paltani & Courvoisier 1997 and references therein). In this framework, Paltani & Courvoisier 1997 were the first to compute variability in the object's rest frame. They found that the variability-versus-luminosity relation is compatible with a power law of slope -0.08. This conclusion does not have a straightforward explanation since a series of discrete, independent (i.e., Poisson distributed) events would produce a slope of $-1/2$ which is incompatible with the observed trend. Paltani & Courvoisier 1997 found that to produce the observed slope with a discrete event model it is necessary to suppose that the parameters describing the properties of the events must depend on the average luminosity of the object.

From a theoretical point of view, time variability is one of the open problems in understanding the active galactic nuclei physics. As matter of fact not only the above-mentioned relationship between variability and luminosity, but even the observed AGN light curves cannot be easily reproduced by theoretical models. For example the classical accretion disk model (Shakura & Sunyaev 1973) fails, since it is difficult to reconcile to the observed variable emission (Courvoisier & Clavel 1991). Even more elaborate models able to produce more realistic spectra by taking into account a hot corona (see e.g. Haardt et al. 1994 and references therein) or comptonization effects (Czerny & Elvis 1987, Ross et al. 1992) have difficulties in explaining the variability features.

To explain both the ultraviolet emission and its variability a completely different type of model has been proposed by Terlevich 1992 and by Courvoisier et al. 1996, hereafter Paper I. These models have the common feature of supposing the AGN emission as a superposition of uncorrelated events, supernovae for the former, star collisions for the case of Paper I. In particular the model presented in Paper I has shown that when a very dense cluster of stars surrounds a super massive black hole the energy released in collisions between stars can be comparable to the luminosity observed in galactic nuclei. In addition these energetic star collisions occur at a rate such that the resulting luminosity is highly variable and similar to the observed light curves.

For the two above mentioned models reproducing the observed shape of the time evolving emission is not a problem. Hence the relationship between variability and luminosity is an important, non trivial, test.

In this framework the analysis presented in this paper has the double purpose of making the stellar collision model of Paper I more realistic and of testing it by comparing its prediction to the variability-luminosity curve.

The paper is organized as follows: the model properties, the criteria of the parameter choice and the emission computation procedure are explained in Sects. 2, 3 and 4, respectively. In Sect. 5 the variability is introduced and its dependence on different parameters is illustrated. In Sect. 6 a comparison between our results and those of Paltani & Courvoisier 1997 is discussed. Sect. 7 analyses the influence of an accretion term on our results and Sect. 8 presents the conclusions.

2. Model properties

In this paper the model presented in Paper I has been improved in different respects. A mass distribution for the stars has been introduced as well as a star radius distribution. A more realistic description of star collisions has been also developed by intro-

Send offprint requests to: torricel@arcetri.astro.it

ducing: i) the angle θ (between the direction of motion of one star and the trajectory of the other one, $0 \leq \theta \leq \pi$ with $\theta = \pi$ corresponding to the case of equal star velocities); ii) the impact parameter b (defined as the smallest distance between the two star centers). The influence of these new parameters is described hereafter.

As a first step, mass segregation has not been taken into account in the expression for the star density distribution (stars/pc^3/dM) which reads:

$$N(R, M)\mathrm{d}M = n(R)M^{-(1+x)}\mathrm{d}M. \quad (1)$$

In this expression x is the Salpeter parameter, R is the distance from the central black hole and M is the star mass in units of the solar mass $M_\odot$, $M_{\min} \leq M \leq M_{\max}$. The spatial distribution of stars $n(R)$ is the same as used in Paper I, namely

$$n(R) = N_0 \left(\frac{R_0}{R + R_0}\right)^k \quad \mathrm{stars/pc}^3. \quad (2)$$

The presence of stars of different masses has important consequences on the energetics of stellar collisions since the energy released in each collision is strictly linked to the amount of the involved mass. In fact, the energy available for emission in the collision between stars M_1 and M_2 (star masses in terms of $M_\odot$) is the star kinetic energy relative to the center of mass:

$$E_* = \frac{1}{2}M_\odot(M_1 + M_2)(v_{\mathrm{k}}^2 - v_{\mathrm{cm}}^2) \ \mathrm{erg}.$$

In this expression v_{cm} is the mass center velocity,

$$v_{\mathrm{cm}}^2 = v_{\mathrm{k}}^2 \left[1 - 2\frac{M_1 M_2}{(M_1 + M_2)^2}(1 + \cos\theta)\right]$$

and $v_{\mathrm{k}}(R)$ is the star keplerian velocity

$$v_{\mathrm{k}}(R) = \sqrt{\frac{G\, M_{\mathrm{Tot}}}{R}} \ \mathrm{cm/sec} \quad (3)$$

around the central mass, M_{Tot}. M_{Tot} is composed of the black hole mass M_{BH} and the sum of all stellar masses inside the sphere of radius R:

$$M_{\mathrm{Tot}}(R) = M_{\mathrm{BH}} + \quad (4)$$
$$+ M_\odot \int_{R_{\mathrm{S}}}^{R} 4\pi R^2 n(R)\, \mathrm{d}R \int_{M_{\min}}^{M_{\max}} M^{-(1+x)}\mathrm{d}M$$

where $R_{\mathrm{S}} = 2GM_{\mathrm{BH}}/c^2$ cm is the Schwarschild radius.

The introduction of a more realistic geometry for star collisions takes into account that the relative velocity of the two stars, v_{rel}, is related to the θ angle:

$$v_{\mathrm{rel}} = 2\, v_{\mathrm{k}} \cos(\theta/2)$$

and that the cross section for a collision is πb^2. Since a collision can occur only if the distance between the two star centers is less or equal to the sum of the two star radii, the impact parameter is limited by the condition

$$0 \leq b \leq \frac{R_{*1} + R_{*2}}{R_\odot}$$

where b is in units of the sun radius, $R_\odot$.

Star radii, R_*, are defined in terms of star masses by the following the relationship (Foellmi 1998)

$$\frac{R_{*\mathrm{i}}}{R_\odot} = \left(\frac{M_{\mathrm{i}}}{M_\odot}\right)^{0.74} \quad (5)$$

obtained from a fit over the results of stellar evolutionary models by Schaller et al. 1992.

Assuming an isotropic distribution of stars, the collision rate within a shell $\mathrm{d}R$ at a distance R from the black hole is

$$\mathrm{d}\tau = 4\pi R_\odot^2 v_{\mathrm{k}} R^2\, n^2(R) \int_{M_{\min}}^{M_{\max}} (M_1 M_2)^{-(1+x)} \times \quad (6)$$
$$\int_0^{\frac{R_{*1}+R_{*2}}{R_\odot}} 2b \int_0^{\pi} 2\cos(\theta/2)\, \mathrm{d}\theta\, \mathrm{d}b\, \mathrm{d}M_1\, \mathrm{d}M_2\, \mathrm{d}R$$

Some of the parameters entering the collision description can not be fixed from outside, these are: the distance R and the time t at which the collision takes place, the masses M_1 and M_2 of the two stars involved, the angle θ between their orbits and the impact parameter b. Even a complete solution of the dynamic of a star cluster around a black hole can not completely define these parameters since initial conditions in the cluster are unknown. In our analysis these parameters have been randomly chosen for each collision taking into account the constraint that the final distribution of each series of parameters must fulfill specific requirements. These requirements are: final mass distribution must follow expression (1); θ and b must have a distributions like $P(b)\mathrm{d}b \propto 2b\ \mathrm{d}b$ and $P(\theta)\ \mathrm{d}\theta \propto 2\cos(\theta/2)\ \mathrm{d}\theta$; R distribution must take into account that the collision probability at distance R is given by the collision rate $\tau(R)$; the time at which collisions occur must follow a Poisson distribution of mean rate τ.

The other parameters present in the above description have been chosen following the physical considerations described hereafter.

3. Parameter choice

3.1. The star density

The star density distribution shown in expression (2) holds for $R \leq R_{\mathrm{ext}}$ while for larger distances $n(R)$ is assumed to have a very steep gradient so that no contribution comes from the regions outside R_{ext}. The choice of the density parameters N_0, R_0 and k is not a trivial one. From the observational point of view no indication exists about the star density profile near galaxy nuclei.

Theoretical models of cluster evolution around a black hole (Bahcall & Wolf 1976, Lightman & Shapiro 1978, Murphy et al. 1991) give more information about the density profile but the number of assumptions used in this procedure recommends to take these values only as a suggestion about the possible parameter ranges. For example, Murphy et al. 1991 starting from a density distribution with a slope R^{-5} for $R >> 1\,pc$ find, after 15 Gyr of evolution, an internal ($R < 0.01\ pc$) slope of $R^{-1/2}$which may become harder ($R^{-7/4}$) in the outer shell

($0.01\ pc \leq R \leq 1\ pc$) if the central black hole mass is smaller than $10^8 M_\odot$.

Since a sure choice of the density parameters is not possible we decided to test our model for different values of k and R_0, namely $k = 0.5, 0.9, 1.5, 2.5$ and $30\ R_{\rm S} \leq R_0 \leq 300\ R_{\rm S}$. $R_{\rm ext}$ has been set equal $10^4 R_{\rm S}$ and N_0 is a free parameter.

3.2. The black hole mass

Black hole masses in active galactic nuclei are usually thought to be in the range 10^6–$10^9 M_\odot$. The central mass amount has different consequences on the structure of our model. First of all the mass value is strictly linked to the typical dimension of the physical system through the scaling parameter $R_{\rm S}$. This fact implies that, for example, a star cluster core extended $100\ R_{\rm S}$ around a black hole of mass $M_{\rm BH} = 10^6 M_\odot$ is only $3\ 10^{13}$ cm wide while that around a black hole of mass $M_{\rm BH} = 10^9 M_\odot$ is $3\ 10^{16}$ cm wide. Such a difference implies a factor 10^9 between the two cluster volumes and, therefore, it will have a non-negligible influence on star collision rate values and on the total number of stars in the cluster. The importance of this point, related with the choice of star density values in the cluster, will be evident in the next section.

The second consequence of a different central mass on the model structure is the following. Our model requires the presence of stars near the central black hole, hence the above mass range must take into account the condition that stars must survive to the black hole tidal effect. Assuming that stars outside $6R_{\rm S}$ must not be disrupted, this new constraint reads

$$6\ R_{\rm S} \geq r_{\rm tidal} = R_* \left(\frac{M_{\rm BH}}{M_*} \right)^{1/3}.$$

Making use of expression (5) and performing a mean over the stellar mass distribution, the above condition becomes

$$M_{\rm BH} \geq 3.2\ 10^6 M_\odot.$$

Since this limit has been obtained by weighting over the mass distribution it does not assure that massive stars orbiting near the black hole are not destroyed. However a more detailed calculation shows that already for $M_{\rm BH} = 10^7 M_\odot$ the fraction of disrupted massive stars inside $10R_{\rm S}$ is less than $5\ 10^{-3}$. Our model is therefore consistent for black hole masses in the range $10^7 M_\odot \leq M_{\rm BH} \leq 10^9 M_\odot$. For lower values of $M_{\rm BH}$ the model should take into account tidal disruption of stars.

3.3. Star mass distribution

The parameters entering the definition of the star mass distribution (Eq. (1)), have been chosen following the classical values, i.e. $x = 1.35$, $M_{\rm min} = 0.1$ and $M_{\rm max} = 120$. Probably near a black hole these values are not the good ones since, for example, an enhanced massive star formation can be supposed (Williams & Perry 1994). However, more suitable values are not known and so we chose to assume these ones and to vary them in a second time to test their influence on the model.

4. The emission

The emission process is the same as outlined in Paper I, to which we refer. For the generic "j" collision the emission $H_{\rm j}$, in erg s^{-1}, is given by the star available kinetic energy, E_*, times a function of the impact parameter which takes into account the efficiency of the process, times a temporal profile:

$$H_{\rm j}(t) = \frac{E_*}{T_{\rm cool}} \left(1 - \frac{bR_\odot}{R_{*1} + R_{*2}} \right)^2 [1 - \cos(2\pi t / T_{\rm cool})].$$

Here the cooling time, $T_{\rm cool}$, is defined as the time the plasma sphere takes to become optically thin:

$$T_{\rm cool} = \frac{1}{v_{\rm exp}} \sqrt{\frac{3M_\odot(M_1 + M_2)}{2\pi m_{\rm p}} \sigma_{\rm T}}\ \ {\rm sec}$$

with $\sigma_{\rm T}$ the Thompson cross section, $v_{\rm exp} = 10^9$ cm s^{-1} the cloud expansion velocity and where it has been assumed that $(M_1 + M_2)$ solar masses of expanding plasma are involved. The possibility of pair creation has been taken into account in deducing $T_{\rm cool}$. It has not been reported here since it does not have influence on the values of the emission variability. How pair creation modifies the emission light curve is shown in Paper I.

If all collisions with all possible combinations of parameters take place, the mean emission in erg s^{-1} will be:

$$H = \int_R \int_\theta \int_b \int_{M_1, M_2} E_* \left(1 - \frac{bR_\odot}{R_{*1} + R_{*2}} \right)^2 {\rm d}\tau. \qquad (7)$$

whose order of magnitude and parameter dependence can be derived as

$$H \simeq v_{\rm k}^2(R_0) M_\odot \tau. \qquad (8)$$

However, in practice we shall only observe the contribution of the collisions which take place in a certain time interval. Hence we can derive the emission light curve adding at each time t the contribution of all J collisions taking place from $R = 6R_{\rm S}$ to $R = R_{\rm ext}$ and having a non-vanishing light curve at that time:

$$H_{\rm coll}(t) = \sum_{\rm j=1}^{\rm J} H_{\rm j}(t)\ {\rm erg\,s^{-1}}.$$

The observed mean luminosity of the source is then

$$L_{\rm coll} = \lim_{t_{\rm Max} \to \infty} \frac{1}{t_{\rm Max}} \int_0^{t_{\rm Max}} H_{\rm coll}\ {\rm d}t\ \ {\rm erg\,s^{-1}}.$$

For a sufficiently large number of collisions $L_{\rm coll}$ clearly approaches H and hence $L_{\rm coll}$ can be approximated, using expression (8), as

$$L_{\rm approx} \simeq H \simeq v_{\rm k}^2(R_0) M_\odot \tau. \qquad (9)$$

In conclusion the procedure used to derive the emission from the star cluster orbiting around the black hole is as follows. For each set of random chosen parameters, i.e. for each collision, the light curve $H_{\rm j}(t)$ is computed. From the sum of all these contributions the overall light curve $H_{\rm coll}(t)$ and the mean luminosity $L_{\rm coll}$ are deduced.

As the approximate expression (9) for the luminosity shows, the mean luminosity value is directly proportional to τ and, on the other hand, the light curve shape obviously depends on the collision rate. In Paper I, the authors arrived to the conclusion that, in order to reproduce the observed AGN features, collision rates in the range $5 < \tau < 50$ collisions/yr are required. An easy but qualitative way to arrive to an analogous conclusion is from variability observations, which report intensity variations on time scales Δt in the range (some year $\gtrsim \Delta t \gtrsim$ 2 days). In the framework in which these intensity variations are due to star collisions occurring at intervals of (2 Δt), it follows $0.5 \lesssim \tau \lesssim 91$ collisions/yr. As an example Fig. 1 shows a light curve with a reasonable value of τ.

Hence, in the scenario in which AGN luminosity variations are explained by means of stellar collisions, the model must account for collision rate values of the order of ten. However, obtaining collision rate values of the order of ten independently of the AGN physical system, i.e. of the central mass amount, is not obvious. To better explain this point the parameter dependence of τ can be derived from expression (6) assuming that the star density is constant inside R_0 and vanishing outside:

$$\tau \propto \int_0^{R_0} N_0^2 \sqrt{\frac{M_{\rm Tot}}{R}} R^2 \mathrm{d}R \propto \sqrt{M_{\rm Tot}} N_0^2 R_0^{2.5}$$

$$\simeq \sqrt{M_{\rm BH}} N_0^2 R_0^{2.5}.$$

So, for different $M_{\rm BH}$ values we can obtain the same τ value using almost identical values of N_0 and R_0 (which means different values of the quantity $\alpha = R_0/R_{\rm S}$) or, if α is fixed, using different values, suitably chosen, of N_0:

$N_0^2 \propto M_{\rm BH}^{-0.5} R_{\rm S}^{-2.5} \propto M_{\rm BH}^{-3}$.

Hence, τ values in the 'good' range can be obtained either changing the system scaled dimensions $R_0/R_{\rm S}$ or the central star density N_0 or both. So the star cluster core extension, if defined in terms of $R_{\rm S}$, will be different in systems with different central masses: we can suppose that the lowest central masses ($M_{\rm BH} = 10^7 M_\odot$, see Sect. 3.2) are related to larger $R_0/R_{\rm S}$ ratios in order to avoid too high star density. For example we obtain the same collision rate $\tau = 5$ collisions/yr for $M_{\rm BH} = 10^7 M_\odot$, $N_0 = 5.6\ 10^{13}$ stars/pc^3, $R_0 = 400\ R_{\rm S}$ and for $M_{\rm BH} = 10^8 M_\odot$, $N_0 = 10^{13}$ stars/pc^3, $R_0 = 100\ R_{\rm S}$. We note that, in spite of the high central star densities, the total number of stars in the two clusters (i.e. stars lying inside the shell of radius $R = R_{\rm ext}$, corresponding to 1 pc for $M_{\rm BH} = 10^7 M_\odot$ and to 10 pc for $M_{\rm BH} = 10^8 M_\odot$) is not a large one, since it is $3.8\ 10^6$ and $2.8\ 10^7$ stars, respectively.

The consequences of the above analysis are twofold: i) high star densities are generally required in order to have suitable τ values; ii) a change in the density parameters N_0 and R_0 can also be representative of a change of the central black hole mass.

5. Emission variability

In order to compare the results of this model to the observed variability values, we derive an explicit expression for this quantity in terms of the parameters of our model.

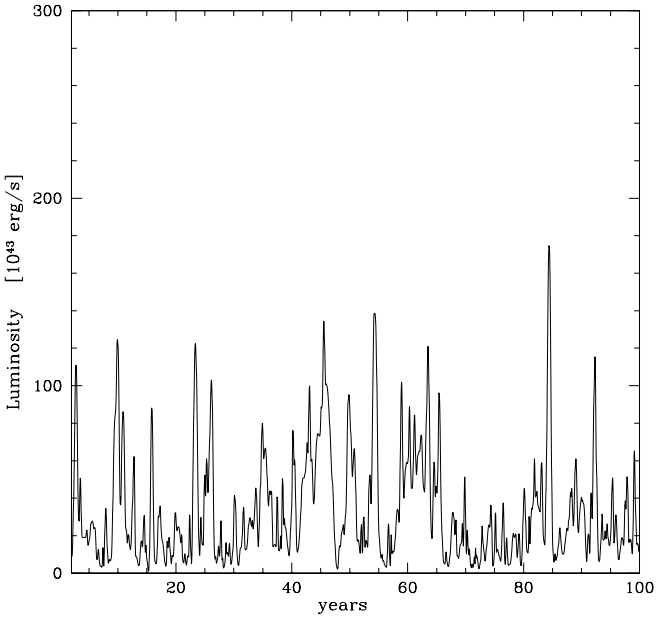

Fig. 1. Light curve for the case of a collision rate $\tau = 12$ and for $k = 2.5$.

The computed light curve $H_{\rm coll}(t)$ can be sampled at $(N-1)$ times intervals, i.e. at times $t_{\rm n}$ with n=1, N and the variability can be derived as

$$\sigma = \frac{1}{L_{\rm coll}} \left[\frac{1}{N-1} \sum_{\rm n=1}^{N} (H_{\rm coll}(t_{\rm n}) - L_{\rm coll})^2 \right]^{1/2.} .$$

This quantity has been numerically computed for different sets of input parameters in order to investigate their influence on the final result. The results of this analysis are described hereafter.

As discussed in the previous section, τ depends on the star density distribution parameters. In each of our computations we have chosen specific values of k, R_0 and $R_{\rm ext}$ and changed that of N_0 in order to have a 'good' τ value. For τ in the 'good' range, the influence of the other parameters on variability and luminosity values are the following:

• Changes in R_0 and k are crucial for the resulting luminosity and variability as described in the following.

• Different values of $R_{\rm ext}$ have been tested in the interval (10^4–$3\ 10^5 R_{\rm S}$); these changes do not influence the results if $k = 1.5$ or $k = 2.5$. For $k < 1$ the external regions of the cluster give a big contribution so as $R_{\rm ext} = 10^4 R_{\rm S}$ has been settled in order to have a reasonable ($< 10^9$) number of stars.

• The effects of changing the value of $M_{\rm BH}$ are more complex. In the framework in which N_0 is freely changed, the presence of a different central mass apparently does not have any effect on $L_{\rm coll}$ and hence on σ. This fact is due to our working hypothesis of selecting a specific interval of τ values. In fact, from the approximate expression (9) it appears that $L_{\rm coll}$ depends only on τ and $v_{\rm k}$. If τ has a value in the 'good' range, independently of $M_{\rm BH}$, $v_{\rm k}^2$ only could show a dependence on the

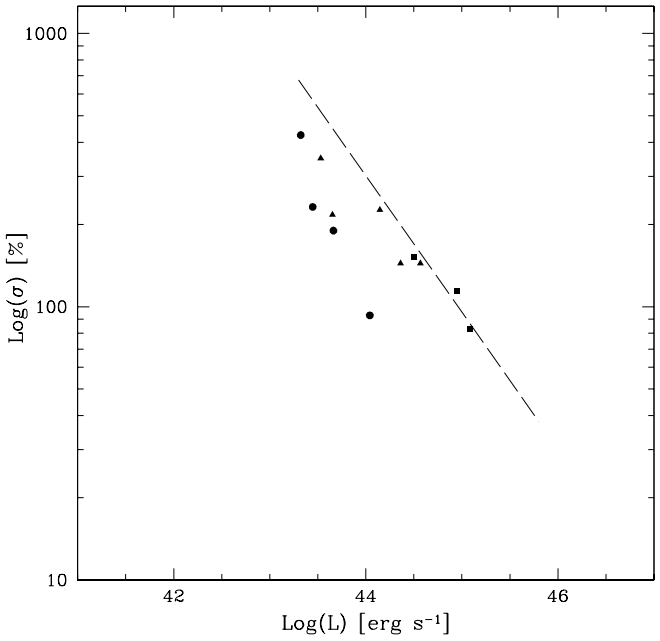

Fig. 2. Variability as a function of $L_{\rm coll}$ for $M_{\rm BH} = 10^8 M_\odot$, $R_{\rm ext} = 10^4 R_{\rm S}$, $k = 2.5$ and different values of R_0. Different symbols correspond to different values of R_0, namely, $R_0 = 30\ R_{\rm S}$ (squares),$R_0 = 100\ R_{\rm S}$ (triangles), $R_0 = 300\ R_{\rm S}$ (circles). The dashed line has slope -1/2.

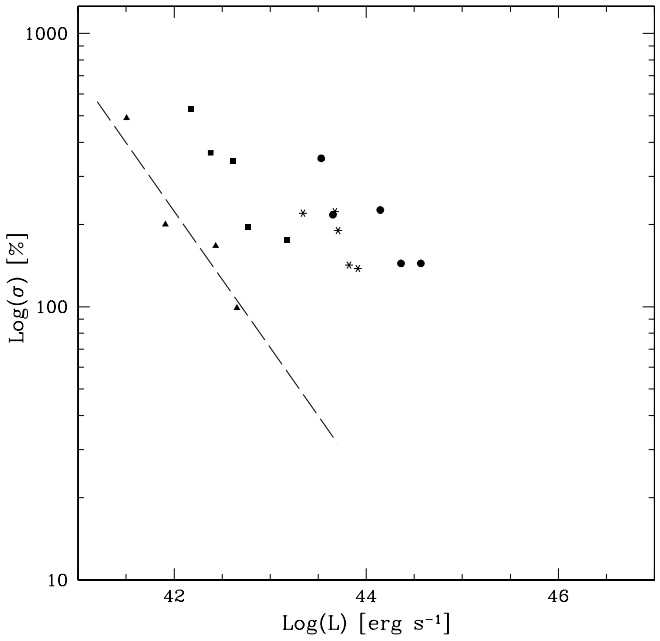

Fig. 3. Variability as a function of $L_{\rm coll}$ for $M_{\rm BH} = 10^8 M_\odot$, $R_{\rm ext} = 10^4 R_{\rm S}$, $R_0 = 100\ R_{\rm S}$ and different values of k. Different symbols correspond to different values of k, namely, $k = 2.5$ (circles), $k = 1.5$ (asterisks), $k = 0.9$ (squares), $k = 0.5$ (triangles). The dashed line has slope -1/2.

black hole mass. However, this is not the case as one can check by rewriting R in Eq. (3) in terms of $R_{\rm S}$ as $R = R_0 = \alpha R_{\rm S}$:

$$v_{\rm k} \propto \sqrt{\frac{M_{\rm Tot}}{\alpha R_{\rm S}}} \simeq \sqrt{\frac{M_{\rm BH}}{\alpha R_{\rm S}}} \propto \sqrt{\frac{M_{\rm BH}}{\alpha M_{\rm BH}}}.$$

As a matter of fact the dependence from the central black hole mass is completely hidden in τ, and through it, in the choice of star density parameter N_0 (see Sect. 4 for details). The same conclusion does not hold for the other possibility presented in Sect. 4, namely that of compensating the change of $M_{\rm BH}$ (i.e., that of $R_{\rm S}$) with that of the ratio $\alpha = R_0/R_{\rm S}$. In fact, in this case α has a different value and hence $v_{\rm k}$ and $L_{\rm coll}$ change. However, this difference is qualitatively analogous to that due to a change in the density distribution which is discussed hereafter and in Sect. 8.

• Changes in the the mass distribution parameters, x, $M_{\rm min}$, $M_{\rm max}$ do not have a sizable influence on σ if the value of N_0 is suitably rearranged.

In conclusion the two parameters which can change the variability value and that of $L_{\rm coll}$ are those which define the shape of star density, i.e. k and R_0 (in which is included the dependence on $M_{\rm BH}$ through the change of $R_{\rm S}$, as discussed above). This means that different density profiles can produce similar collision rates but different luminosities and variabilities. Looking again at the approximate expression (9) the above conclusion can be easily understood. In fact, for equal τ values, a different star distribution implies different average velocities of the colliding stars and therefore a different amount of the available energy, $L_{\rm coll}$. Hence the more the star distribution is concentrated around the center, the higher the luminosity. This fact can be confirmed by Figs. 2 and 3 where it is shown how σ and $L_{\rm coll}$ depend on the parameters k and R_0. In both figures the points on the right hand side of the picture correspond to more peaked star distributions i.e. to the distributions having the smallest R_0 (Fig. 2) or the steepest profile (Fig. 3).

In order to obtain Figs. 2 and 3 N_0 values have been chosen, for each pair (k, R_0), so as the values of τ result in the range (1–15). This fact implies that the values of N_0 used for Figs. 2 and 3 are in the range $10^{11} - 10^{14.3}\ M_\odot/pc^3$. These values are very high if compared with the star density observed in the center of our galaxy. However, the context here is different, since in this model we are dealing with active galaxies in which we presume that the activity itself is due to the presence of a great number of stars near the galaxy center. In this context the high star concentration is a necessary ingredient of the model and the star density value can be lower only around very massive black holes, i.e. when the typical dimension of the system ($R_{\rm S}$) increases.

In Figs. 2 and 3 a straight line of slope -1/2 has been drawn. As it has been explained in the introduction, this is the slope expected from a series of independent discrete events. It is evident from the above figures that each group of points obtained varying N_0 for a specific pair (k, R_0), is aligned along a line with the same slope -1/2. A small scatter, presumably due to the procedure of random choice of some parameters, is present. This alignment confirms the correctness of all the treatment since it shows that, when increasing the event number (i.e. N_0 in our case), the expected relationship for a discrete event model is found.

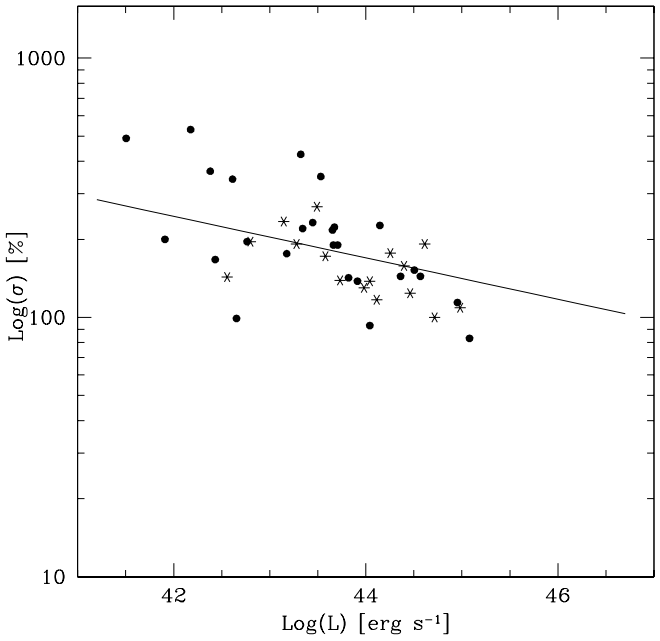

Fig. 4. Variability as a function of $L_{\rm coll}$ for $M_{\rm BH} = 10^8 M_\odot$, $R_{\rm ext} = 10^4 R_{\rm S}$ and: *a)* all the pairs (k, R_0) shown in Figs. 2 and 3 [dots]; *b)* a series of pairs (k, R_0) corresponding to density configurations with $\tau = 10$ [asterisks]. The straight line has the same slope of that shown in Fig. 1 of Paltani & Courvoisier 1997

6. Results

In Figs. 2 and 3 the results have been presented so as to make evident the dependence on different parameters. It is obvious that the star density distribution in real galaxies is not a universal quantity. It will depend on the nature of the galaxy itself and on its age, as theoretical evolutive models also show (see e.g. Murphy et al. 1991). Therefore, to compare our results to those derived by Paltani & Courvoisier 1997 we have reported in Fig. 4 the luminosity and variability values corresponding to a variety of different pairs of k and R_0, namely all those present in Figs. 2 and 3 plus a series of pairs (k,R_0) corresponding to density configurations having a collision rate $\tau = 10$. A straight line with the same slope as that Paltani & Courvoisier 1997 derived as approximative trend of σ as a function of $L_{\rm coll}$ has been also reported in Fig. 4. This straight line has been arbitrarily shifted since, as described in the introduction, it is the trend which is important in this comparison. On the other hand a detailed comparison between our results and those by Paltani & Courvoisier 1997 would imply the non-evident task of relating the luminosity and the light curve observed at a specific wave length with the spectral integrated luminosity and light curve derived here.

The straight line with slope -0.08 is compatible with the points drawn in Fig. 4. It is however important to understand how much this result depends on the parameter choice. In this figure different pairs (k, R_0) have been reported for a restricted choice of the collision rate value ($1 < \tau < 15$) and we know from Sect. 5 that the results are not influenced by other free parameters of the model. Hence the only possibility is that the allowed range in τ, or equivalently that in N_0, causes the compatibility between the points of Fig. 4 and the straight line with slope -0.08 derived by Paltani & Courvoisier 1997.

To test if the compatibility is real, we have added to the pairs previously computed the results obtained for the case of sixteen different configurations having the same collision rate $\tau = 10$. For these sixteen additional cases, marked in Fig. 4 by asterisks, the Spearman's correlation coefficient is equal to -0.63. The probability to get such a high correlation coefficient for 16 pairs of quantities belonging to two uncorrelated groups is less than 0.011. We conclude that the correlation is most probably real. This correlation proves that the compatibility of all points drawn in Fig. 4 with the line of slope -0.08 does not depend on the choice of τ values, since such a compatibility still exists for a single τ value.

7. The accretion emission

To this point the colliding star model does not take into account the fate of all matter ejected by star collisions into the region around the black hole. It is not our purpose to perform here a detailed physics of this matter evolution and emission. Nevertheless, it is important to test here if and how much this plasma can change the results of the previous section.

We can easily suppose that part of the plasma ejected into the interstellar medium can stream along different planes towards the central black hole and can be accreted. In this framework two different emission contributions would be present: the hot expanding shells of plasma caused by star collisions and the accretion of the same plasma on the central black hole.

The second emission process can be taken into account supposing that in each collision about $(M_\odot/2)$ of plasma goes, once cooled, into accretion, producing energy with a conversion efficiency assumed to be about 0.05. Since the collision rate is τ, the overall emission due to accretion is:

$$L_{\rm acc} = 0.05 c^2 \frac{M_\odot}{2} \tau.$$

This picture, although very simplified, can give an order of magnitude of this process even if the real accretion luminosity would be probably lower (since we have chosen an upper limit for the amount of accreting matter) and varying in time (since matter is discontinually injected into the interstellar medium).

It is important to take into account that this approximate treatment is self consistent only if the typical accretion time $(1/\tau)$ is longer than the matter free fall time on the black hole, i.e. if holds

$$\tau < 1.5\ 10^{12} \frac{M_\odot}{M_{\rm BH}} \left(\frac{R_0}{R_{\rm S}}\right)^{-3/2} = \tau_{\rm Max}. \qquad (10)$$

If the mean luminosity due to collisions is approximatively expressed as in Eq. (9) and expression (3) is taken into account, the above expression for $L_{\rm acc}$ can be rewritten as

$$L_{\rm acc} \simeq 0.025 \frac{c^2}{v_{\rm k}^2} L_{\rm coll} \simeq 0.025 \frac{R_0}{R_{\rm S}} L_{\rm coll} \qquad (11)$$

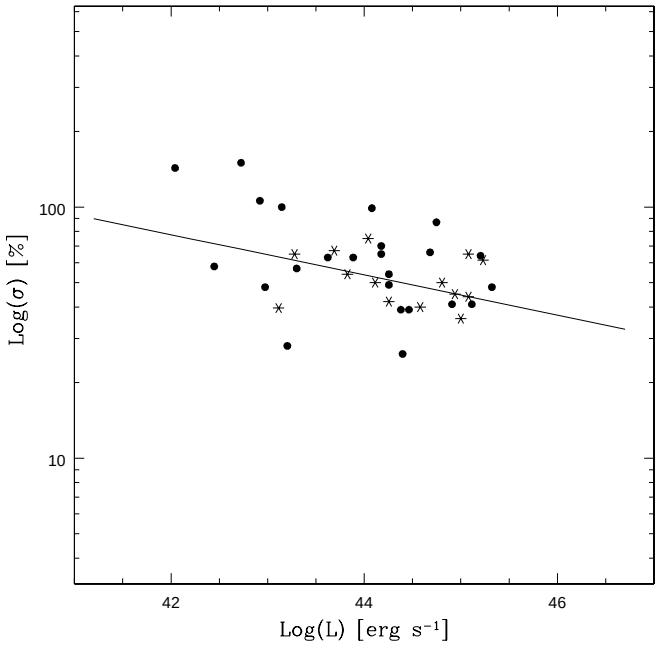

Fig. 5. Variability as a function of $L_{\rm coll}$ for $M_{\rm BH} = 10^8 M_\odot$, $R_{\rm ext} = 10^4 R_{\rm S}$ and: *a)* all the pairs (k, R_0) shown in Figs. 2 and 3 [dots]; *b)* a series of pairs (k, R_0) corresponding to density configurations with $\tau = 10$ [asterisks]. Pairs (k, R_0) corresponding to density configurations with $\tau > \tau_{\rm Max}$ have been rejected. The straight line has the same slope of that shown in Fig. 1 of Paltani & Courvoisier 1997

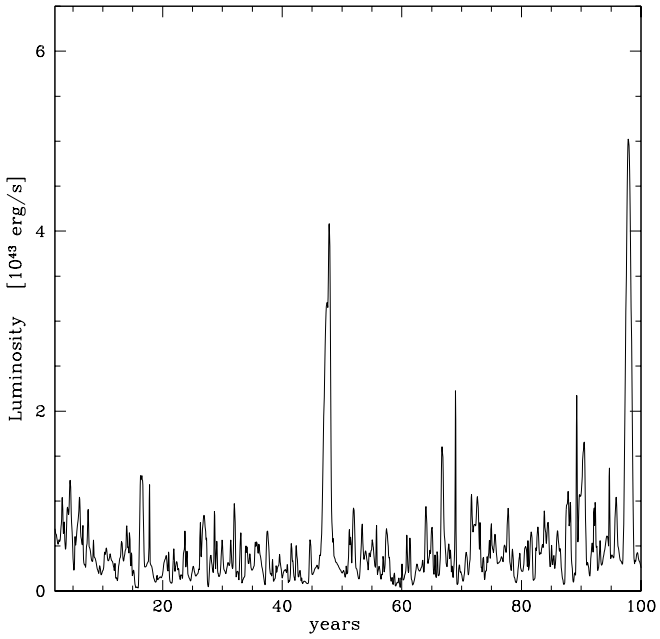

Fig. 6. Light curve for the case of collision rate $\tau = 12$ and for $k = 0.5$.

and the total observable luminosity results

$$L_{\rm tot} = L_{\rm coll} + L_{\rm acc} \ \ {\rm erg\,s^{-1}}.$$

With this new expression for the cluster emission we have performed the same computations as in the case without accretion. The same parameter sets have been used with the only exception that those pairs (k, R_0) which did not fulfill the upper limit for τ of Eq. (10) have been rejected. So the reported results correspond to parameter values for which it results $1 < \tau < \tau_{\rm Max}$. The results are shown in Fig. 5. In this case, because of noise, we cannot state the compatibility of luminosity versus variability values with a line of specific slope. However, it is important to note that the introduction of the accretion component (even if in an approximated form) does not prevent the possibility of the previous found compatibility with the line of slope (-0.08).

8. Discussion and conclusions

The analysis of this paper is based on the working hypothesis that AGN variability is due to star collisions occurring in the neighborhood of the central black hole. These collisions will reproduce the observed AGN luminosities (in the range $10^{42} - 10^{46}$ erg s^{-1}) and light curves only if their rate, τ, is such that more than one (and no more than one hundred) collisions occur every year. A fixed range in τ values implies a definite relationship among the dimensions of the star cluster, its density and the mass of the central black hole (see Sect. 4); high central star densities are required especially around black holes with masses approaching the smallest allowed value ($10^7 M_\odot$). In this framework the theoretically derived variability values are compatible with the observational results of Paltani & Courvoisier 1997. More in detail, as it is apparent from Fig. 4, the results of our analysis clearly do not follow the slope -1/2 (typic of a series of discrete, independent events), but reproduce very well the observed trend in spite of the simplicity and of the strong approximations of the model. A more detailed and realistic physics both of star collisions and of matter accretion can change the variability values but can not change this trend. In addition the dispersion of theoretical points in Fig. 4 is analogous to that present in the experimental data shown in Paltani & Courvoisier 1997. A fact which simply reflects the existence of different stars distributions in different galaxies.

It is also important to stress that the agreement between our results and those of Paltani & Courvoisier 1997 is not due to the presence of many parameters in the model, since most of them, as explained in Sect. 5, do not influence the result shown in Fig. 4. In fact, the dispersion of the points in Fig. 4 is only due to different concentrations of stars near the galaxy center, which induce different distributions of collision energies (see Sect. 5). This means that the model presented here is able to fit observations because of the form of the keplerian velocity. Peaked density distributions favor high velocity stars and hence strong collisions. The difference in the event intensity can be estimated by comparing the light curves corresponding to two different configurations present in Fig. 4 having the same collision rate value but different density distribution. The first one is the light curve of Fig. 1; the second one is shown in Fig. 6. The two curves are generated with the same collision rate $\tau = 12$ and hence both have a shape compatible with the observed AGN light curves. A difference in the star density distribution ($k = 2.5$ and $k = 0.5$,

respectively) produces a big difference in the collision intensity and hence in the produced luminosity, as the vertical scales of the two figures show.

Acknowledgements. This work was partly supported by the Italian Ministry for University and Research (MURST) under grant Cofin98-02-32

References

Bahcall J.N., Wolf R.A., 1976, ApJ 209, 214
Courvoisier T.J.-L., Clavel J., 1991, A&A 248, 389
Courvoisier T.J.-L., Paltani S., Walter R., 1996, A&A 308, L17 – Paper I
Czerny B., Elvis M., 1987, ApJ 321, 305
Foellmi C., 1998, Travail de diplôme, Université de Genève
Haardt F., Maraschi L., Ghisellini G., 1994, ApJ 432, L95
Lightman A.P., Shapiro S.L., 1978, Rev. Mod. Phys. 50, 437
Murphy B.W., Cohn H.N., Durisen R.H., 1991, ApJ 370, 60
Paltani S., Courvoisier T.J.-L., 1997, A&A 323, 717
Schaller G., Schaerer D., Meynet G., Maeder A., 1992, A&AS 96, 269
Shakura N.I., Sunyaev R.A., 1973, A&A 24, 337
Ross R.R., Fabian A.C., Mineshige S., 1992, MNRAS 258, 189
Terlevich R., 1992, In: Filipenko A.V. (ed.) Relationships between Active Galactic Nuclei and Starburst Galaxies. ASP Conf. Ser. Vol. 31, ASP, San Francisco
Williams R.J.R., Perry J.J., 1994, MNRAS 269, 538